Bucket Operation

This is the third section of our insight into valvetrain design and it looks at valvetrain dynamics. It has been sub-divided into two parts, A and B and this first part covers valvetrain dynamics for a direct acting bucket tappet. As ever our guides are Prof. Gordon Blair, CBE, FREng of Prof. Blair & Associates, Charles D. McCartan, MEng, PhD of Queen's University Belfast and Hans Hermann of Hans Hermann Engineering.

THE FUNDAMENTALS

When one opens up the program for 'cam design and manufacture' in the 4stHEAD software [1] the user is faced with the following quotation from the writers of this computer package. It is as follows: "There is no such thing as cam design, there is only valve lift profile design which requires the creation of a cam and follower mechanism to reliably provide this designed valve lift profile."

In Part One of this article in Race Engine Technology 009, we described the creation of valve lift profiles. In Part Two (Race Engine Technology 010) we described the "creation of a cam and follower mechanism to reliably provide this designed valve lift profile". In the process we used a relatively simple dynamic analysis of the mechanism to compute the Hertz stresses and oil film characteristics at the cam and follower interface. The analytic technique employed there was not sufficiently detailed as to ensure that the phrase 'reliably provide this designed valve lift profile' was completely satisfied. Here we delve deeply into the dynamic behaviour of the cam and follower mechanism to show how this design process is completed.

Due to the sheer extent of this particular subject area it has not proved possible to do so in any meaningful way in a single article in one issue of Race Engine Technology, as the reader was initially promised by the authors. In view of this we have split it into two parts, Part 3A and Part 3B. Here, in Part 3A, we examine the valvetrain dynamics of the relatively simple case of bucket tappets, the most common of direct acting cam follower mechanisms. In Part 3B we shall look in detail at the most difficult of all dynamic cases, the pushrod mechanism with particular reference to the NASCAR engine.

THE BUCKET TAPPET CAM FOLLOWER MECHANISM

In Fig.1 is shown a cutaway picture of a direct-acting cam follower mechanism in the form of a bucket tappet acting on a valve restrained by valve springs. You can see that the bottom coil of the spring is "closed and ground" to hold it square with the cylinder head and the valve spring retainer, as the technical phrase has it, and becomes a "dead coil" exerting no spring pressure on the valve. Normally there is a single dead coil at each end of the spring, but the actual non-integer numbers of these coils are counted and used as computation data. The spring coils which move and are compressed on deflection by valve lift are known as the "active" coils.

Valve springs come in a variety of shapes, wire types and wire materials. Wire materials may be Cr-Si steel, Cr-Va steel, stainless steel, or titanium and the computation must be able to cope with any particular material selection. Wire types can be of a round or ovate cross-section. The winding of the spring can produce a parallel spring with equal diameter coils and with even spring spacing which usually exhibits a constant spring stiffness with deflection. The winding of a spring can also produce a parallel spring with equal diameter coils but with unequal spring spacing. This will have an increasing spring stiffness with deflection and is known as a 'progressive' spring. Yet another type of spring winding can produce a tapered spring with unequal diameter coils and unequal spring spacing which will also have an increasing spring stiffness with deflection. This can be either a 'conical spring' in one format or a 'beehive spring' depending on the outer profile of the windings. The computation must be able to ingest and use the data for any and all of these springs.

For example, the Fig.2 shows the information sketch for the input data for the more complex case of a 'tapered spring with ovate wire' where further input data on individual spring spacing and individual coil diameter is also required. Although the input data sheet asks the user to enter the measured values of (initial) spring stiffness and spring mass, a high-quality computation will actually calculate such data for any wire material selected and compute not only the natural frequency of the spring but the changing spring stiffness with deflection if it happens to be 'progressive'. In short, accurate valvetrain design software should be able to design the valve springs as well as compute their effect on the valvetrain dynamics [1].

THE MATHEMATICAL MODEL OF THE BUCKET TAPPET VALVETRAIN

A simple mathematical model of a bucket tappet valvetrain is shown in Fig.3. This picture will cause many a reader to recall with horror their 'vibration' lectures at university, not to speak of the awkward second order differential equations that arose from it which were almost unsolvable under examination conditions!

This simple model lumps the masses of the valve, retainer and ➤

tappet into a single mass. The total valve spring mass is set between the two halves of a (double stiffness) spring with (velocity related) dampers located as shown. This level of complexity of mathematical model is relatively easily solved on today's PC but the output data from it is quite inadequate for valvetrain design purposes. This deficiency arises because one has no knowledge of the movement of the individual coils of the spring so that the spring stress levels cannot be accurately computed nor can there be any information available on the bounce of the valve on and off its valve seat, nor any data regarding possible separation of the tappet from the cam. As the entire purpose of valvetrain dynamics analysis is the computation of that very data, a more detailed mathematical model is required. It is shown in Fig.4.

The principal difference between the mathematical models in Fig.3 and Fig.4 is that:

(a) separation and bounce of all components is possible where all such locations are marked by a circled 'S' or circled 'B';

(b) each active coil of each valve spring(s) is computed as a separate spring-mass-damper system;

(c) the bucket tappet surface can deflect with load and is treated as a spring-mass-damper system;

(d) the valve stem and the valve head masses are computed as separate spring-mass-damper systems;

(e) the cam and camshaft can deflect and are calculated as a spring-mass-damper system;

(f) when the valve bounces on the valve seat and cylinder head that process incorporates the stiffness of the cylinder head and valve seat within the computation.

You will observe in Fig.4 that there are damping coefficients used for every spring-mass-damper system within the computation. Damping coefficients are not dimensionless but have the units of force/velocity, or Ns/mm in the case of the 4stHEAD software [1]. The literature on valvetrain dynamics is almost entirely bereft of experimental data to use as input data numbers for damping coefficients within such a computation. Considering that we have been 'designing' valvetrains for internal combustion engines for over a century, this tells us that not only has this been a sparse research area but it is also one that has mathematically daunted most engineers until more recent times when the computer could accomplish what the slide rule could not. In Part 3B of this article we hope to show some of the experimental work we are doing on this very subject.

THE VALVE LIFT PROFILES FOR A BUCKET TAPPET VALVETRAIN

In parts 1 and 2 of this article [2, 3] we designed various valve lift profiles and showed how to design and manufacture the cams for various follower mechanisms. Two of these valve lift profiles, Designs A and D, were characterised as being 'moderately aggressive' and 'very

Fig.1 The cam, cam tappet, valve, and valve springs.

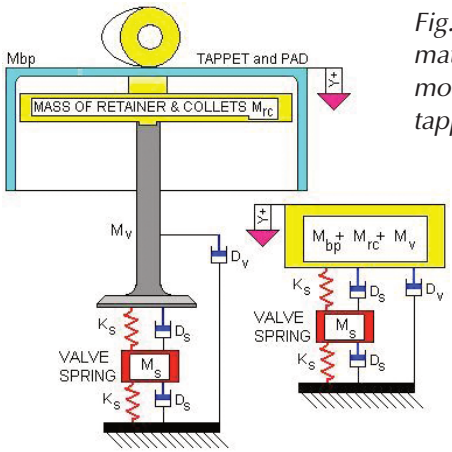

Fig.3 A simple mathematical model for a bucket tappet system.

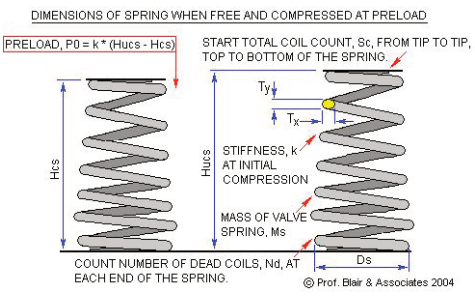

Fig.2 Some of the input data requirements for valve springs.

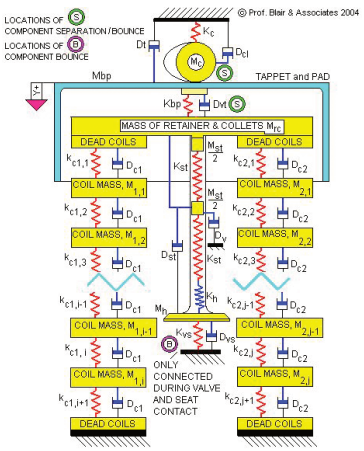

Fig.4 A complex mathematical model for a bucket tappet system.

aggressive', respectively, and suitable for use only with direct acting (bucket tappet) or rocker or finger cam followers.

Design E was 'less aggressive' and was stated as being much more suitable for a pushrod follower mechanism while Designs A and D were stated as being unsuitable for that application. You will have to await Part 3B to read about pushrod valvetrain dynamics and the accuracy, or otherwise, of those statements. Here we will examine the valvetrain dynamics of a bucket tappet mechanism exposed to these same three valve lift profiles.

You will recall that each valve lift profile had a total lift of 10.3 mm with a duration of 150 cam degrees above a 0.3 mm ramp lift so that the nominal valve lift was 10.0 mm above that ramp. If the hot valve lash clearance is set to 0.2 mm, then the actual valve lift is 10.1 mm and the valve lift duration is 161 deg and the initial cam to bucket contact occurs on the constant velocity section of the ramp.

THE VALVE FOR A BUCKET TAPPET VALVETRAIN

We have 'designed' a suitable valve for this hypothetical valve train. It is shown drawn to scale by the software in Fig.5 from input dimensions as specified in Fig.6. To give you feeling for scale, the outer seat diameter, Dos, is 30 mm.

Also specified as input data is the material for the manufacture of this valve. If the material is specified as titanium, then the mass of the valve is computed as 21.4 g and the stiffness of the stem, Kst, is 29859 N/mm and the stiffness of the valve head, Kh, is 28740 N/mm. If the material is specified as steel, then the mass of the valve is computed as 36.8 g and the stiffness of the stem, Kst, is 49744 N/mm and the stiffness of the valve head, Kh, is 47900 N/mm.

Valve head stiffness is remarkably sensitive to minor dimensional changes. For example, if the corner radius, Rvh in Fig.6, is halved from the original value of 7 mm to 3.5 mm, the stiffness of this same titanium valve head, Kh, drops from 28740 to 9118 N/mm.

THE BUCKET TAPPET

In a similar vein, we have 'designed' a suitable bucket tappet for our hypothetical valve train. The information for the input data is shown in Fig.7 and the software draws to scale a sketch of this bucket tappet and its pad, which is seen in Fig.8. The outer diameter of the bucket, Db, is 28.5 mm and its sidewall thickness, Tw, is 1 mm. The bucket is calculated to weigh 22 g and its stiffness is 28047 N/mm. The bucket tappet and pad are normally made from steel but other materials may be selected within the software for either component. ➤

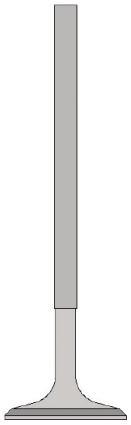

Fig.5 A scaled sketch of the valve used in the discussion.

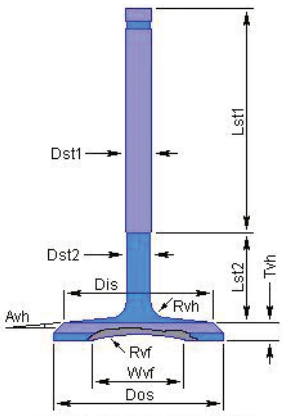

Fig.6 Some of the input data requirements for the valve.

Fig.7 Some of the input data requirements for the bucket.

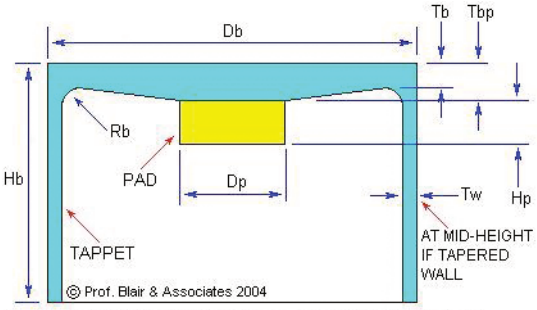

Fig.8 A scaled sketch of the bucket used in the discussion.

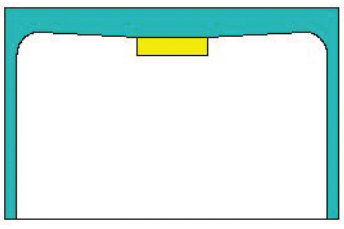

input data for main valve spring	
number of coils Sc	5.75
mass of valve spring Ms (g)	22.7
free spring height Hucs (mm)	36
preload spring height Hcs (mm)	29
spring outside diameter Ds (mm)	26
spring wire diameter Ts (mm)	3.1
spring stiffness k (N/mm)	19.6
number of dead coils at each end Nd	1
spring coils damping Dc (Ns/mm)	0.008
input data for inner valve spring	
number of coils Sn	6.97
mass of valve spring Ms (g)	10.3
free spring height Hucs (mm)	34
preload spring height Hcs (mm)	27
spring outside diameter Ds (mm)	19.0
spring wire diameter Ts (mm)	2.2
spring stiffness k (N/mm)	9.5
number of dead coils at each end Nd	1
spring coils damping Dc (Ns/mm)	0.008

Fig.9 Some of the input data for both valve springs.

Fig.10 Movie snapshot of the valve springs at zero lift.

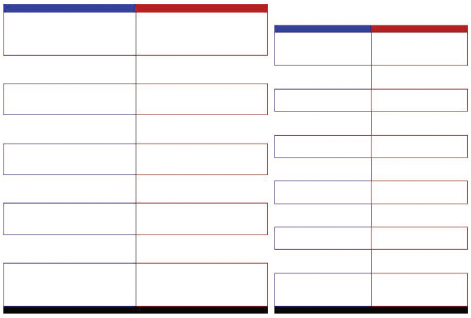

Fig.11 Dynamic minus static valve lift for Designs A-E.

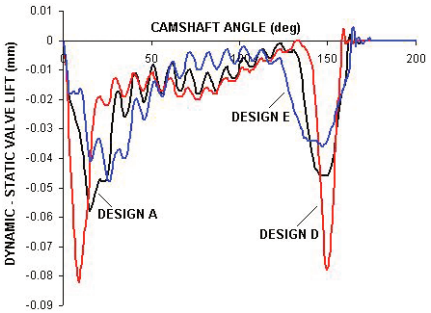

Fig.12 Cam to bucket tappet forces for Designs A-E.

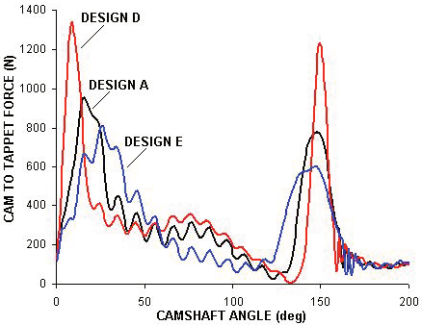

THE VALVE SPRINGS

The valve springs are created within the 4stHEAD software and the salient dimensions of the outer and inner springs are shown in Fig.9 with reference to the nomenclature of Fig.2, although as these are parallel wound, round wire springs the ovate dimensions of Tx and Ty devolve to a single wire diameter, Ts. The wire material is selected as Cr-Si steel. The software post-processor creates a movie of the static and dynamic motion of the valve spring. Prior to motion, it is drawn as a scaled sketch of the valve springs with the inner spring, if there is one, extracted and set to the right for clarity, as in Fig.10. The active coils are shown at their centre of mass, but the spring is drawn in two halves, a blue-coloured half in which the spring coils are going to move as if statically and a red-coloured half spring which will be seen to move dynamically [1].

MORE VALVETRAIN INPUT DATA

We will not bore you with further valvetrain input data such as the camshaft mass and its stiffness but one item of input data is important. With a titanium valve and the input data as above, the valvetrain performed quite satisfactorily in the motoring mode, i.e., as if driven by an electric motor, up to 4750 camshaft cycles/min or 9500 engine rpm. It did so for all three imposed valve lift profiles through the cam, Designs A-E. We propose to show you the dynamic results at 4750 cam rpm for a successful valvetrain design.

DYNAMIC VALVETRAIN ANALYSIS AT 4750 RPM WITH A TITANIUM VALVE

Here the valvetrain with the bucket tappet is operating successfully and it is important that we first show you what is considered to be relatively stable dynamic conditions before discussing instability.

The dynamic and static valve lift graphs are almost identical, so we will not waste space by showing them, but in Fig.11 is plotted the difference between the dynamic and static valve lift. The three graphs show this data for the three valve lift Designs A-E. The largest valve under-lift is due to component strain from the fastest valve acceleration which is Design D, but the valve bounce at the reseating point for all three cases is virtually identical and amounts to no more than 0.01 mm. The high frequency oscillation along each graph is due to the natural frequency of the cam and camshaft system arising from the mass, Mc, and stiffness, Kc, assigned to those components through the nomenclature of Fig.4.

When the cam-to-tappet forces are plotted in Fig.12 for valve lift Designs A-E it can be seen that the highest force, and hence the largest strain on the tappet, is due to Design D. As the valve nears reseating at about 140 deg, this force falls to zero so the potential for cam-to-tappet float is looming large.

In Figs.13-15 are shown the dynamic and static valve accelerations for valve lift Designs A-E and the static data is

Fig.13 Dynamic and static valve acceleration for Design A.

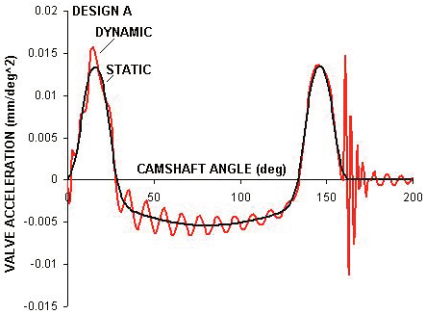

Fig.14 Dynamic and static valve acceleration for Design D.

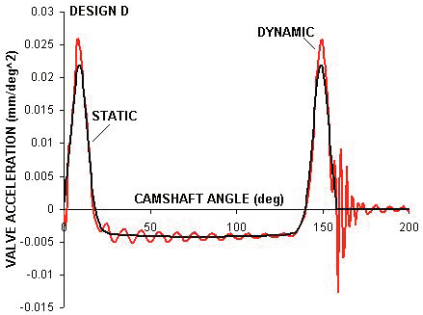

Fig.15 Dynamic and static valve acceleration for Design E.

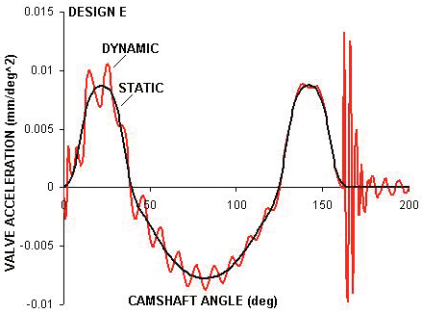

Fig.16 Top and bottom valve spring coil forces for Design A.

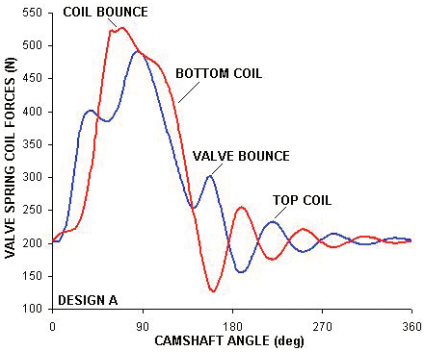

exactly as we presented it in Part 1 [2]. Although the dynamic acceleration closely follows the static acceleration, with an overlay of that already-seen high frequency oscillation, the main point to note is the large accelerations that occur as the valve bounces with the most minimal bounce levels of 0.01 mm or less. These oscillations are as large in amplitude as the positive spring coil (in red) experiences higher forces than the top coil and, by definition, higher stresses which is why parallel springs, if they fail, normally crack at the bottom coils.

This happens because the bottom coil is fully compressed, that spring coil is fully bent and twisted, and so records the highest stress. It bounces off the dead coil and the sharp bounce is

> "The main point to note is the large accelerations that occur as the valve bounces with the most minimal bounce levels of 0.01 mm or less"

static acceleration but the force is mostly absorbed by the valve head and, as the valve has bounced clear of the tappet, it barely shows up on the cam-tappet forces in Fig.12.

The valve bounce, however minimal, does show up on Figs.16-18, where the forces on the top and bottom coils of the main valve spring are displayed for valve lift Designs A-E, respectively. The blip on the top spring coil graph (in blue) from 140 to 160 deg is caused by this modest valve bounce and all coils then continue to oscillate at their natural frequency until the valve lifts again. It is, naturally, a sharper blip for the more aggressive valve lift Design D. The bottom indicated on each of Figs.16-18. A snapshot from the software movie in Fig.19 (for Design D) at full valve lift for both spring coils illustrates this point; it is the companion snapshot at full lift to the zero lift picture shown in Fig.10; a full movie of this behaviour can be downloaded from the 'web' [1].

DYNAMIC VALVETRAIN ANALYSIS AT 5400 CAMSHAFT RPM WITH A TITANIUM VALVE

Using valve lift Design D, and retaining all other numerical input data to the computation but with one exception, namely that the ➤

Fig.17 Top and bottom valve spring coil forces for Design D.

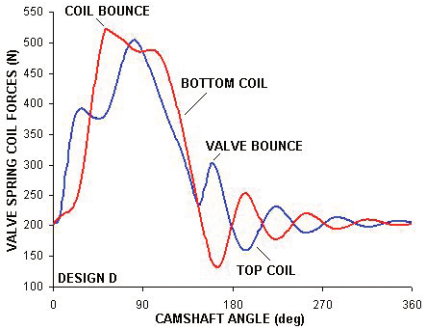

Fig.18 Top and bottom valve spring coil forces for Design E.

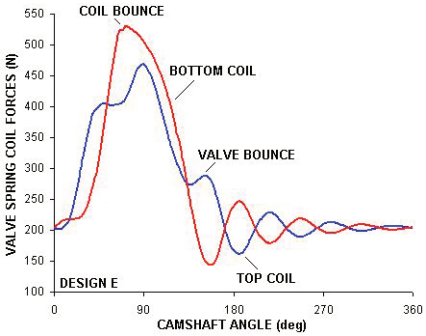

Fig.19 Movie snapshot of the valve springs at full lift.

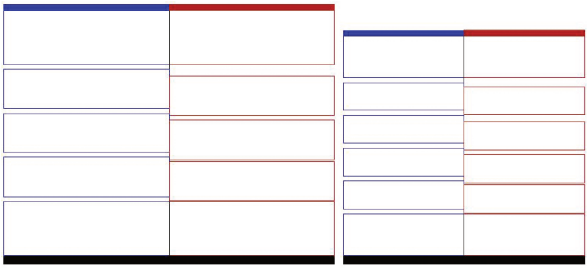

Fig.20 Dynamic and static valve lift for Design D at 5400 rpm.

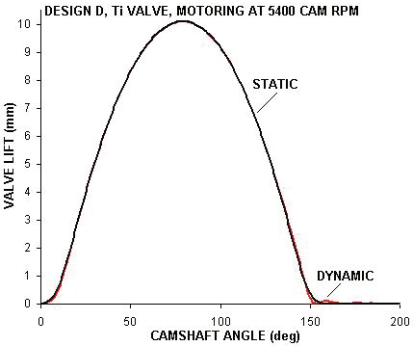

camshaft rotation speed is raised to 5400 rpm (10,800 rpm crankshaft) from 4750 rpm (9500 rpm crankshaft), the calculation is repeated. Unstable valvetrain dynamics is now observed. The valvetrain is being computationally motored in both cases, i.e., as if driven externally on an experimental vibration test rig.

In Fig.20 is shown the static and dynamic valve lift at this higher engine speed. Valve bounce can be seen as the valve tries to reseat itself.

A close-up of the valve bounce area is given in Fig.21 where the dynamic valve has floated (lofted) above the static lift curve but forcibly re-establishes contact with the cam at about 147 deg.

This heavy contact tries to force the valve to reverse its direction of motion, eventually doing so at 154 deg. The ensuing valve bounce reaches a value of some 0.1 mm at 159 deg before banging down again at 165 deg on to the valve seat. It hits the valve seat because the valve and tappet cannot hit the cam at this juncture as the valve lift period is now concluded. The strain energy stored is then released again at 171 deg to give another bounce for 9 deg duration and yet again at 182 deg for a 5 deg duration. The physical contact of the cam with its tappet is broken after 158 deg when the static lift goes to zero and the bucket is 'free' to oscillate between the valve and the base circle of the camshaft.

This process is further illuminated by output data from the computation on the float of the bucket tappet away from the cam; this is found in Fig.22. The lofting of the valve and tappet as earlier noted starts at 120 deg but is dramatically ended at 147 deg as the valve and tappet under-lift and hit the cam. Between 147 deg and 154 deg the tappet float off the cam is zero as it is pushed hard against the valve, but between 155 and 166 deg when the valve bounces so the bucket floats off the cam. A similar picture of tappet float takes place between 171 and 180 deg as the valve bounces for the second time.

Reinforcement for this information comes in Fig.23, giving the cam to tappet forces over this same period. As the valve lofts and the bucket floats between 120 and 147 deg the cam to tappet force is zero. However, during the lift reversal before the first 'bounce', between 147 and 155 deg, the cam to tappet force increases to 2315 N. This force is 31% higher than the 1765 N maximum force found during an earlier segment of the dynamic valve lift. Under stable conditions, see Fig.12, the closing force at the same juncture only rose to 1235 N.

The instability seen in Fig.23 is very much a shock load and is clearly going to significantly elevate the Hertz stress level at the cam and tappet interface. A similar picture of elevated contact forces, when the tappet float is zero, is seen for the 166 to 172 period and for the 180 to 182 period. In Fig.21 the valve bounce periods correspond to the bucket tappet float periods and to the zero cam tappet force periods, namely 155 to 166 deg, 172 to 180 deg, and 182 to 187 deg.

Perhaps the most important point to make is that it is not

Fig.21 Close-up of dynamic valve bounce for Design D at 5400 rpm.

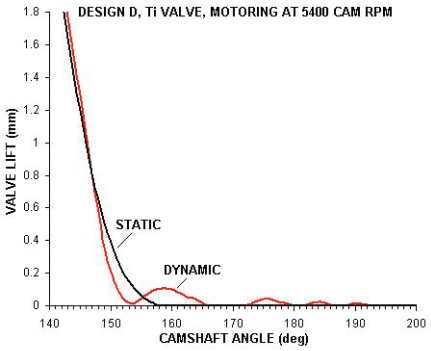

Fig.22 Float of the bucket tappet for Design D at 5400 rpm.

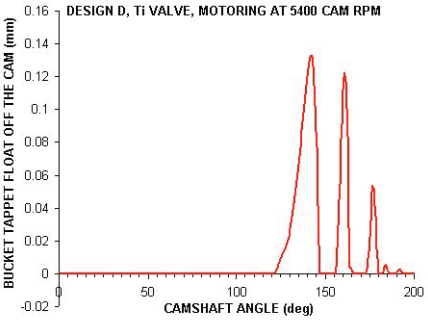

Fig.23 Cam to bucket tappet force for Design D at 5400 rpm.

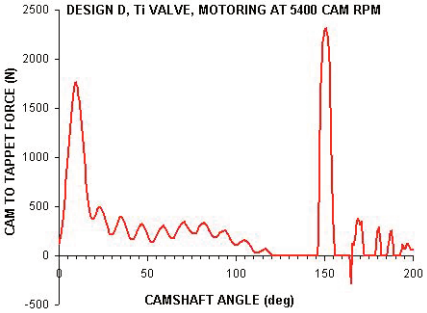

Fig.24 Valve accelerations for Design D at 5400 rpm.

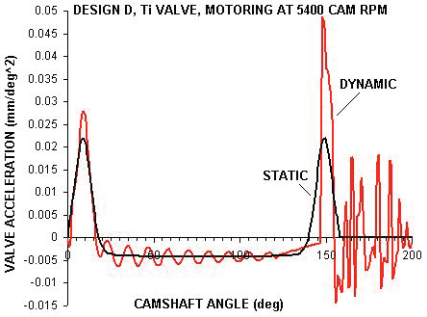

the valve bounce that gives a dramatic spike on the cam to tappet force. It is the first lift reversal as the springs propel the valve back towards its seat from a 'lofting' position (here from 147 to 155 deg). The cam to tappet forces in the subsequent intervals between valve bounces are much lower. The potential damage that the valve bounce provides is to expose valve flow area between the engine cylinder and its ducting and that has repercussions for the engine's breathing ability; but of that more below.

In Fig.24 is shown the static and dynamic acceleration of the valve head. The positive acceleration spike between 147 and 155 deg corresponds precisely with the spike on the cam to tappet force of Fig.23. The violent high frequency shaking that the valve head experiences during the subsequent valve bounce periods should not be discounted in mechanical damage terms as they may well eventually encourage a thoroughly-fatigued valve head to seek a quieter life elsewhere, not connected to its valve stem!

The more violent dynamic acceleration picture at 5400 cam rpm can be contrasted and compared with the calmer equivalent scene in Fig.14 when the camshaft speed is 4750 rpm. The peak positive acceleration on the 'spike' of Fig.24 is exactly double that of the closing positive acceleration of Fig.14. Acceleration, you will recall, is directly related to force and in Fig.12, for valve lift Design D, the peak value is just 1235 N but here in Fig.23 it is 2315 N, as you could have predicted.

DYNAMIC VALVETRAIN ANALYSIS UNDER FIRING CONDITIONS AT 5400 RPM

Using exactly the same input data as for the motoring case above, the computation is repeated but with the major difference that the valve head is exposed to the actual cylinder pressure conditions over a complete 360 cam deg cycle. In the 4stHEAD software it is possible to realistically recreate virtually any cylinder pressure characteristic from a turbo-diesel to a lawnmower. The one that is used for this computation mimics a naturally aspirated engine with a well-tuned intake and exhaust system.

The peak pressure is set at 78 bar and the imep created is 14.8 bar with a pumping mep of 0.7 bar. A plot of a segment of this cylinder pressure, below 5 bar or during the breathing cycle, is shown in Fig.25. Depending on whether one elects to mimic an exhaust valve or an intake valve, the face of the valve head will experience a pressure upon it appropriate to that particular operational period. The back of the valve head will then feel a pressure upon it as a function of the gas flow direction, whether that flow is sonic or subsonic, etc. The dynamic force on the valve head at any juncture is then basically the difference between these two pressures multiplied by the area of the head of the valve. To illustrate the point that a tuned, naturally aspirated engine is the focus of this particular simulation, note the drop in cylinder pressure from intake valve opening, IVO, to exhaust valve closing, EVC, in Fig.25. ➤

Fig.25 Cylinder pressure used for the firing conditions.

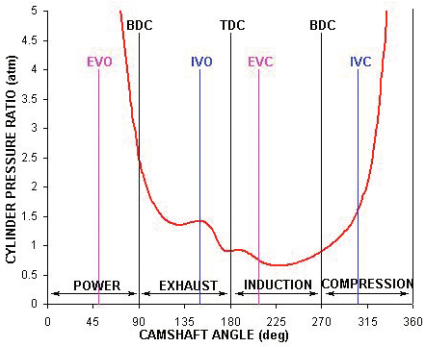

Fig.26 Initial intake and exhaust valve lift if firing conditions.

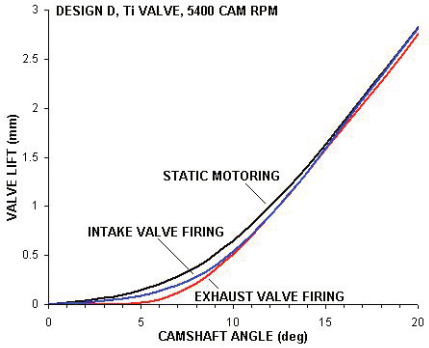

Fig.27 Final intake and exhaust valve lift if firing conditions.

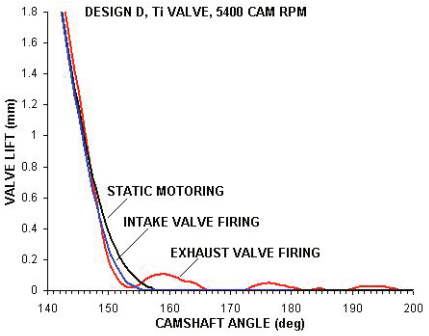

Fig.28 Peak intake and exhaust valve lift if firing conditions.

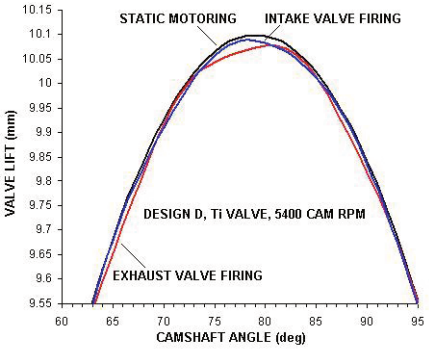

Without going into every detail of the simulation output, as with the motoring case, the major differences between the motoring and the firing case are shown in Figs.26-28 and they are significant. On each diagram the static valve lift is shown in 'black', the exhaust valve in 'red', and the intake valve in 'blue'. For this particular behavioural comparison, the size of the exhaust and intake valves are assumed to be identical but in reality this would rarely be the case.

In Fig.26 is given a close-up of the dynamic valve lift behaviour for the first 3 mm of valve lift. The intake valve lifts in an almost identical fashion to the motoring case, with some under-lift due to system strain and bending for some 17 deg before it matches that of the static lift. The exhaust valve, opposed by a cylinder pressure ratio of some 10 atm over its 30 mm diameter giving a force of some 715 N, fails to move at all until some 4 or 5 deg have passed, or 10 deg at the crankshaft.

In Fig.27 is shown the situation at the closing of the valves. At first glance, the bounce of the exhaust valve looks very similar to that of the motoring case but a closer comparison with Fig.21 reveals that the bounce periods during firing are longer and the third major bounce in the firing case is much higher and later. The later bounces are exaggerated because the falling cylinder pressure tends to suck the exhaust valve open. The intake valve, on the other hand, does not bounce at all due to the rapidly rising cylinder pressure on the compression stroke opposing the valve bounce motion.

In Fig.28, around the peak valve lift period, the under-lift of the exhaust valve persists and the location of peak lift is retarded by some 3 deg camshaft, or 6 deg crankshaft. The peak lift of the intake valve is advanced by some 2 deg due to the action of the sub-atmospheric cylinder pressure upon it.

One of the many reasons for the study of valvetrain dynamics is to export to an accurate engine simulation [3] the dynamic valve lifts of the intake and exhaust valves so that it may predict more precisely the engine breathing characteristics and, ultimately, the engine performance characteristics. The folly of conducting such an engine simulation with static valve lift curves is obvious but the folly of doing so with dynamic valve lift curves acquired under motoring conditions, either by computation as exemplified by Figs.20-24 or by experiment on a valvetrain motoring rig, is now equally obvious from the evidence of Figs.25-28.

The extra exhaust valve bounce of the firing case occurs during induction so an accurate engine simulation will record an enhanced ingestion of exhaust gas and compute its effect on engine performance. The retarded opening of the exhaust valve under firing conditions will hamper exhaust outflow and raise the pumping loss on the exhaust stroke. Depending on the particular design, the lack of bounce of the intake valve at closure could either reduce cylinder back flow of already-ingested air and raise the Delivery Ratio, or it could lessen the intake ramming effect and potentially lower the Delivery Ratio.

Fig.29 Various unstable valvetrain dynamics for Design D.

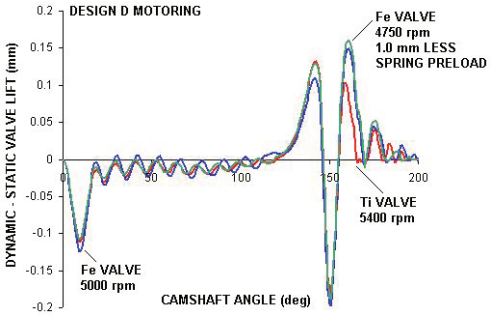

The experimental acquisition of dynamic valve lift curves under firing conditions on an engine is a most difficult exercise and one that is prone to both magnitude and phase shift errors. Even if it is accurate, it is an expensive way to discover at such a late stage that the dynamic valve lift characteristics are unacceptably poor in terms of either lift or bounce. It is clearly more logical to employ a computation for valvetrain dynamics under firing conditions in order to optimise the valvetrain design either before conducting the firing engine experiment, or before using engine simulation software to optimise the engine performance characteristics.

MORE ON DYNAMIC VALVETRAIN ANALYSIS UNDER MOTORING CONDITIONS

It was shown above, when discussing the Figs.11-19, that stable dynamic running of this particular titanium valve and bucket tappet mechanism occurred at 4750 camshaft rpm (9500 rpm engine). It was also shown above, when discussing the Figs.20-24, that dynamic instability of this same valve and mechanism happened at 5400 camshaft rpm (10,800 rpm engine). This will be good news for the designer if the objective is to locate peak engine power at 9500 rpm and not at 10,800 rpm and disastrous if the reverse is the aim. However, dynamic valvetrain instability is shown in Fig.29 to occur under other circumstances at camshaft speeds lower than 5400 rpm.

In Fig.29, in 'red', is the difference between dynamic and static lift for the very same case discussed in Figs.20-24 for the titanium valve at 5400 rpm. The valve under-lift between 147 and 155 deg that causes the high cam-to-tappet force is clearly shown as is the first major valve bounce up to 0.1 mm. However, two further cases that produce worse effects are also plotted in Fig.29.

If the titanium valve is replaced with a steel valve the valve mass is increased from 21.4 g to 36.8 g, or 72% higher and if this computation is run at 5000 rpm the valve bounce increases to 0.14 mm.

If the titanium valve is replaced with a steel valve and the valve spring preload is reduced by 1 mm from 7 to 6 mm and if this computation is run at 4750 rpm, the valve bounce increases further to 0.16 mm. You will recall that 4750 rpm is the very same camshaft speed that provided stable valvetrain characteristics with the titanium valve.

The sensitivity of a valvetrain to relatively minor changes of input data is really quite remarkable and we have often been surprised during a design process by such changes producing dynamic instability. However, it must be emphasised that an unsophisticated valvetrain computation model, particularly one that does not permit component separation and bounce, will not be so sensitive or, in the simple case of the Fig.3 model, not even sensitive at all.

CONCLUSIONS

It is possible today to model valvetrain dynamics with some considerable accuracy provided that the mathematical model is sufficiently extensive. In this brief discussion of the subject much has been left unwritten. Damping coefficients have been highlighted as a topic to be discussed in Part 3B of this article. The use of valve springs other than parallel, round wire springs has not been described other than that the 4stHEAD software can accomplish it. The stresses within the valve spring coils as a result of stable or unstable valvetrain dynamics have not been discussed nor have the desirable, or undesirable, effects of using valve springs of identical or dissimilar natural frequencies been described. Worse, we have not shown the Fourier analyses of the dynamic valve accelerations and their comparison with the original static data. We apologise for some or all of these deficiencies but this article is already long enough. Perhaps we can do better in Part 3b of this article on valvetrain dynamics when we delve in to the much more difficult subject area of pushrod followers for NASCAR-type engines. ■

REFERENCES

[1] 4stHEAD design software, Prof. Blair and Associates, Belfast, Northern Ireland (see www.profblairandassociates.com).

[2] G.P. Blair, C.D. McCartan, H. Hermann, "The Right Lift", Race Engine Technology, Issue 009, July 2005 (see www.racetechmag.com and also www.profblairandassociates.com).

[3] G.P. Blair, C.D. McCartan, H. Hermann, "Making the Right Cam", Race Engine Technology, Issue 010, September 2005 (see www.racetechmag.com and also www.profblairandassociates.com).

[4] VIRTUAL ENGINES Engine Simulation Software, VIRTUAL 4-Stroke and VIRTUAL 2-Stroke, Optimum Power Technology, Bridgeville, PA. (see www.optimum-power.com)